TECHNOLOGIE 5G

Bulletin de veille scientifique : Avril 2026

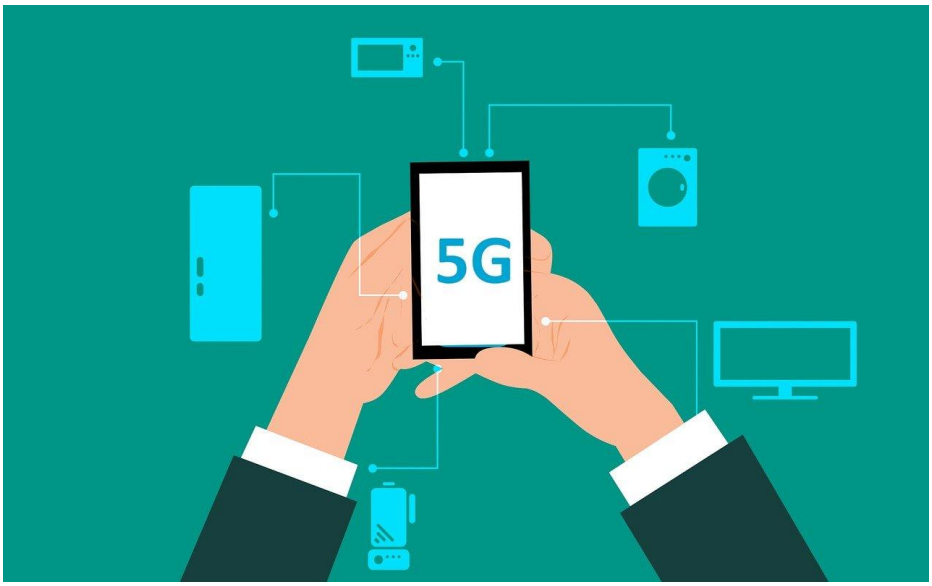

Objectifs : réaliser une veille scientifique sur la technologie 5G

La validation des informations fournies (exactitude, fiabilité, pertinence par rapport aux principes de prévention, etc.) est du ressort des auteurs des articles signalés dans la veille. Les informations ne sont pas le reflet de la position de l'INRS. Les éléments issus de cette veille sont fournis sans garantie d'exhaustivité. Les liens mentionnés dans le bulletin donnent accès aux documents sous réserve d'un abonnement à la ressource.

Les bulletins de veille sont disponibles sur le portail documentaire de l'INRS. L'abonnement permet de recevoir une alerte mail lors de la publication d'un nouveau bulletin (bouton « M'abonner » disponible après connexion à son compte).

Généralités

Aucun article dans ce bulletin.

Performances et sécurité

Low-Altitude Target Localization Method Based on Exogenous Radar with Multi-Base Station and 5G SSB Signals.

Xu Y, Tu G, Zhang L, Zhou Y, Xiong M, Li Y. *Sensors (Basel)*. 2026 Apr 1;26(7).

In this work, we propose a localization method based on an exogenous radar with multi-base station and the synchronization signal block (SSB) in 5G downlink signals. We combine physical cell identities (PCIs)-based identification with the extensive cancellation algorithm (ECA) to reconstruct and cancel the present strongest SSB signal, thereby obtaining reference signal receiving power (RSRP) values of them in descending order of strength. Then, we designed a two-stage localization method. Firstly, we determined the target's coarse location based on the directional characteristics of different SSB beams. Subsequently, we compared the RSRP values extracted from the actually received signals against those pre-obtained when the target is at various reference points. The reference point corresponding to the closest match was selected as the estimated target position. We conducted simulations under various signal-to-noise ratio (SNR) levels, reference point densities, and signal jitter conditions. The simulation results demonstrate that the method outperforms techniques such as Fang's method for time difference of arrival (Fang-TDOA) and observed time difference of arrival (OTDOA).

Lien vers l'article

Machine learning driven clustering for silhouetting 5G network throughput.

Ramesh P, Bhuvaneswari PTV. *Sci Rep*. 2026 Mar 30;16(1).

Compared with previous generations, the 5G enhanced mobile broadband (eMBB) application delivers higher connection, quicker data speeds, and better customer support. Improving data transmission speeds for 5G uplink user equipment (UE) users is the goal of this study. Python is used for data analysis and framework building. This research looks at a 250-m-radius Picocell Base Station (PBS) that can have 15 user equipment (UEs). The position of the user is determined by the cell-range Poisson distribution. The physical base station (PBS), which assesses the state of the signal transmission channel, receives channel state information (CSI) from user equipment (UE). Rayleigh, Rician, free space path, and long-distance route loss models are used in the study. A dataset of channel statuses is generated by the query. There is dynamism in the dataset. K-means clustering is used by UEs to handle service-specific needs. By integrating bandwidth, clustering improves system performance and maximizes the cumulative rate of all user equipment. Channel gain, transmission rate, and minimum service information rate are the characteristics that define UEs. After grouping, users in Cluster 3 had the highest cumulative rate of 9.52 Mbps and an average rate of 7.52 Mbps. In addition to increasing system capacity, bandwidth concatenation satisfied the service needs for every user's equipment (UE). Performance criteria of several clustering models were evaluated, and K-means was found to be the best method. The method was methodically created to satisfy the goals of the study. This research investigates beamforming capabilities and adaptive clustering to improve user fairness and efficiency.

Lien vers l'article

Optimizing 5G NR link layer parameters for eMBB and URLLC applications under dynamic channel and transmission configurations.

Pateriya S, Bandopadhaya S, Bairwa AK, Jain V. *Sci Rep*. 2026 Apr 2.

1000 frames were simulated in MATLAB-based 5G NR link-layer evaluations under 3GPP-compliant conditions to guarantee good statistical reliability. Under realistic propagation conditions, the study concentrated on the following: Downlink shared Channel (DLSCH), Physical Uplink Shared Channel (PUSCH), Physical Uplink Control Channel (PUCCH), Physical Downlink Shared Channel (PDSCH) and Hybrid Automatic Repeat Request (HARQ). The impacts of multipath delay spread, Doppler shifts, and user mobility were captured using standardized channel models, such as CDL-A to CDL-D and TDL-B100. The study looked at dynamically changing transmission parameters, such as frequency-hopping strategies, subcarrier spacings between 15 and 120 kHz, and modulation schemes ranging from QPSK to 256-QAM. The findings showed that while larger subcarrier spacings (60-120 kHz) improved throughput in high-SNR and low-latency scenarios, smaller subcarrier spacings (15-30 kHz) provided better block error rate (BLER) performance in low-SNR and high-delay conditions. Moreover, QPSK proved resilient in noisy settings, whereas 256-QAM reached maximum throughput in favourable SNR conditions. Interestingly, PUCCH with interest frequency hopping had the lowest BLER, demonstrating that it works well in channels that are dominated by fading. The results highlight how important adaptive link-layer configurations are for optimizing spectral efficiency and guaranteeing dependable performance in a range of deployment circumstances. To meet the demanding needs of ultra-reliable low-latency communication (URLLC) and enhanced mobile broadband (eMBB) services in next-generation wireless networks, these insights are essential.

Lien vers l'article

Quantum-resilient cross-trust evaluation for zero trust 5G security.

Jeysuriya K, Renjith PN, Sudhakaran G. *Sci Rep*. 2026 Mar 29;16(1).

The growing complexity of multi-domain 5G networks exposes critical trust and authentication vulnerabilities that traditional security models cannot address, especially against emerging quantum-era threats. In this paper, we propose the Quantum-Resilient Cross Domain Trust Zero Trust Architecture (QCT-ZTA) model to address end-to-end resilience. Integrating blockchain-based federated trust management systems, cross-chain trust negotiations, and post-quantum cryptography will ensure optimal interoperability and resilience. This framework introduces a Quantum-Resilient Proof-of-Trust (QR-PoT) and dynamic cross domain trust scoring systems that mitigate Sybil, Denial of Service, and poisoning attacks. We utilized OMNeT++, Hyperledger Fabric, and liboqs for post-quantum cryptography to implement and evaluate the model on the 5G-NIDD dataset. The results show 88% accuracy in trust detection, a three-fold decrease in unauthorized access, and 35% better throughput stability, compared to the state-of-the-art models Zero-X and TQFL. This proves that QCT-ZTA provides a scalable and quantum-secure trust architecture that is compliant with the 5G and next-generation 6G infrastructures.

Lien vers l'article

Wideband patch antenna with enhanced gain stability for sub-6 GHz 5G applications.

Vijayadheeswar Reddy S, Kumar J. *Sci Rep*. 2026 Apr 2.

The increasing demand for compact, wideband and efficient antennas in 5G sub-6 GHz networks has driven research toward designs offering stable gain and high radiation performance within limited dimensions. This paper presents a gain stabilized wideband patch antenna developed through a systematic six-stage design approach incorporating circular parasitic stubs, L-slots, a meandered feed line and a defected ground structure. These elements interactively work for the provision of multi-frequency impedance matching and the introduction of resonance modes takes place with further extension of the effective electrical length of the circular parasitic stubs, whereas the L-slots are used for the perturbation of the surface currents. The meandered feed line further elongates the current path, lowering the fundamental resonance frequency by 49% without physical size increase. The defected ground structure disrupts ground plane currents, creating capacitive loading that fine-tunes impedance matching and suppresses higher order modes, collectively enabling wideband operation with minimal gain variation. The optimized design exhibits dual resonances at 3.6 and 6.1 GHz with return losses of - 44 and - 27 dB respectively, covering a wide operational band of 3.2-6.6 GHz. The antenna maintains a consistent realized gain of 2.6-2.7 dBi (± 0.8 dB), radiation efficiency above 90%, group delay variation below 0.5 ns and a low quality factor ([Formula: see text]). The novelty lies in the systematic integration of these complementary techniques to simultaneously achieve wideband operation, exceptional gain stability and low group delay, making it suitable for compact 5G wireless devices.

Lien vers l'article

Quad-band SIW antenna with micro-pocket enabled frequency-agile design for 5G/6G IoT applications.

Vaishali P, Dash SKK, Barik RK, Khan MJ, Dewangan NK. *Sci Rep*. 2026 Mar 28;16(1).

A single polarized substrate integrated waveguide (SIW) cavity supported self-quadruplexing antenna, designed for 5G/6G IoT applications is proposed and prototyped. The model is backed by a rectangular substrate integrated waveguide (RSIW) cavity and features four resonating patches excited separately through four different 50Ω feed lines. The antenna center frequencies are obtained at 3.29 GHz, 4.47 GHz, 5.85 GHz, and 7.07 GHz. Additionally, the cavity is engineered with four sets of micro pockets beneath the patches which can be filled with different materials to offer frequency-agile response. The operating frequencies can be tuned over a wide range between 3.29 GHz and 8.4 GHz as per the required targets. The layout of the model is chosen meticulously to ensure all ports are co-polarized and isolation between any two is better than 32 dB. The proposed antenna design exhibits competitive performances with a compact size of 0.09 $\lambda(g)^2$, Front-To-Back-Ratio (FTBR) above 17.83 dB and peak gain of 7.6 dBi. Importantly, all ports are single polarized for the first time in their class. The performance is validated by an equivalent circuit model and prototype characterization. The proposed antenna specifications and configurations well suit for future high-end applications like IoT/5G/6G/satellite communications.

Lien vers l'article

ML assisted optimization of DR based MIMO antenna for 5G communication systems.

Sumit, Kumar V, Pandey A, Sharma A, Ranjan P, Tripathi R. *Sci Rep*. 2026 Apr 10.

This work presents a dual-port cylindrical dielectric resonator antenna (CDRA) based MIMO design for 27-GHz 5G communication, assisted by a suspended complementary split-ring resonator (CSRR) metasurface for port decoupling.
We are providing an unedited version of this manuscript to give early access to its findings. Before final publication, the manuscript will undergo further editing. Please note there may be errors present which affect the content, and all legal disclaimers apply.

Lien vers l'article

Performance evaluation and validation of a quad-element super-wideband fractal MIMO antenna with integrated quad-band filtering capability for advanced 5G/IoT systems.

Sohi AK, Kumar GN, Singh AK, Addepalli T, Zakaria Z, Al-Gburi AJA. *Sci Rep*. 2026 Apr 27;16(1).

This research focuses on the design, simulation, and experimental validation of a four-port, fractal-loaded multiple-input multiple-output (MIMO) antenna to facilitate super-wideband (SWB) operation while suppressing undesired narrowband interference. The array design is prototyped on a cost-effective, 0.464λ(o) × 0.285λ(o) × 0.013λ(o) (at 2.4 GHz) FR4 sheet. The top FR4 layer comprises four metallic hexagonal patches defected with a windmill-inspired rhombus fractal (2nd -order) pattern. At the same time, its rear side features a shared, multi-slotted ground combined with a hexagonal isolator. The designed array effectively transforms the fractal-induced multi-band into a 2.4–25 GHz SWB spectrum (164.96% fractional bandwidth) and significantly attenuates the cross-coupling between the array elements. The designed fractal minimizes the metallic radiator area by 48% compared to the conventional patch with a hexagonal configuration. Moreover, to ensure distortion-free communication, various undesired narrow bands, including downlink/uplink C-band (3.663–4.19 GHz/5.843–6.663 GHz), INSAT (4.48–4.87 GHz), and radio-location (8.969–10.51 GHz), are notched by integrating each array unit with two L-type slits, a rectangular split ring resonator (SRR) pair, and a modified complementary SRR. To assess performance in complex scenarios, the diversity measures are evaluated and observed to conform to their specified thresholds, thereby affirming the conformity between simulated and tested outcomes. Therefore, the designed SWB array facilitates the intrinsic interference immunity for seamless 5G/IoT communication in highly dense propagation environments.

Lien vers l'article

High gain and slant dual-polarized antenna for private 5G railway base stations.

Lee JG, Han Y, Ahn BK. *Sci Rep*. 2026 Mar 26.

This paper proposes a novel antenna structure that simultaneously satisfies high gain, dual-polarization, and fan-beam radiation pattern characteristics for Private 5G base stations in next-generation railway communications. In Private 5G railway communications, a balance of high gain, dual-polarization, and fan-beam is crucial. High gain and fan-beam pattern maximize coverage along the track, while dual-polarization provides link robustness for high-speed mobility. The proposed antenna element achieves a high gain of 12.8 dBi and stable radiation performance despite its relatively compact size by employing a radiation mechanism based on a higher-order mode patch

antenna and a sidelobe suppression technique utilizing central and side slots. Furthermore, by rotating the antenna by 45[Formula: see text] and configuring it in a slant dual-polarization structure, it provides robustness against polarization variations that frequently occur in practical communication environments. A 6 × 1 array antenna constructed based on the proposed antenna element forms a stable fan-beam radiation pattern with suppressed grating lobes even at wide array spacing of 1.27[Formula: see text], providing a horizontal half-power beamwidth (HPBW) of 6[Formula: see text], a vertical HPBW of 38[Formula: see text], and a peak gain of 18.6 dBi. The 6-way power divider designed for dual-polarization array feeding ensures excellent uniform power distribution with an insertion loss deviation within ± 0.32 dB and an insertion phase deviation within ± 2.8[Formula: see text]. Both the proposed antenna element and the array antenna achieve sufficient bandwidth coverage for the Private 5G band, demonstrating performance suitable for application in practical base station environments. Moreover, a figure-of-merit comparison defined based on peak gain, fractional bandwidth, and antenna size confirms that the proposed antenna achieves the most balanced performance compared to previously reported high gain dual-polarized antennas. These results indicate that the proposed antenna can provide high reliability for next-generation Private 5G railway base stations and offer significant advantages in terms of coverage, interference mitigation, and link robustness in practical railway operating environments.

Lien vers l'article

A scalable UWB-to-reconfigurable MIMO filtenna with single-varactor tuning and enhanced isolation for adaptive 5G and cognitive radio systems.

Fouda HS, Hamoud AS, Attia MA. *Sci Rep*. 2026 Feb 13;16(1):6525.

This work presents a complete development framework that begins with a new fork-shaped ultra wideband (UWB) antenna. The antenna is designed, optimized, fabricated, and experimentally validated. The prototype achieves a very wide bandwidth extending from 2.4 to 8 GHz, with stable radiation behavior and high efficiency. Building on this design, a 4 × 4 UWB MIMO array is developed. The four elements are arranged orthogonally to enhance isolation and provide strong pattern diversity. Next, the UWB antenna is transformed into a frequency-reconfigurable filtering antenna (filtenna). A single varactor diode is embedded in a modified radiator to enable continuous tuning from 2.45 to 3.48 GHz. A stepped ground, inset feed, and RF-choke-based biasing network are added to achieve stable tuning and low-loss filtering. The fabricated prototype shows a clear frequency shift with excellent matching and good radiation efficiency. To extend the concept, 2 × 2 and 4 × 4 MIMO filtenna configurations are also developed. Each stage introduces further structural refinement, including inter-element decoupling lines, L-shaped ground extensions, π-shaped shared ground sections, and pairwise high-impedance biasing networks. These features significantly enhance isolation and suppress surface-wave coupling. The proposed MIMO designs provide outstanding diversity performance. An envelope correlation coefficient (ECC) of approximately 10(−2), a diversity gain close to 10 dB, and a channel capacity loss of less than 0.1 bits/s/Hz are accomplished. Additionally, the antenna exhibits deep total active reflection coefficient (TARC) nulls near − 15 dB, along with mean effective gain (MEG) values that are well-balanced around − 3 dB. Taken as a whole, the results confirm that the developed UWB antenna, its reconfigurable filtenna derivative, and their 2 × 2 and 4 × 4 MIMO extensions form a compact, low-loss, and highly efficient solution for next-generation 5G and cognitive radio systems.

Lien vers l'article

Correction: A scalable UWB-to-reconfigurable MIMO filtenna with single-varactor tuning and enhanced isolation for adaptive 5G and cognitive radio systems.

Fouda HS, Hamoud AS, Attia MA. *Sci Rep*. 2026 Apr 9;16(1).

In the original version of this Article, Amal S. Hamoud was omitted as a corresponding author. Correspondence and requests for materials should also be addressed to: PG_189490@f-eng.tanta.edu.eg.
The original Article has been corrected.

Lien vers l'article

Compact Modified Quatrefoil-Shaped Antenna with Dual-Circularly Polarized 28/38 GHz for 5G and Beyond Millimeter-Wave Applications.

Farahat AE, Hussein KFA. *Sensors (Basel)*. 2026 Mar 17;26(6).

This paper presents a compact dual-band circularly polarized (CP) antenna designed for millimeter-wave applications at 28 and 38 GHz, which are critical for emerging 5G and beyond wireless communication systems. The single-element antenna features an ultra-small radiating patch of size 3.34 mm × 3.34 mm and overall substrate footprint of 8 mm × 16 mm, implemented on a Rogers RO3003 substrate with a relative permittivity of 3 and thickness of 0.25 mm, making it highly suitable for space-constrained millimeter-wave front-end integration. Circular polarization is successfully achieved at both bands, with measured axial ratios of 1.4 dB at 28 GHz and 2.2 dB at 38 GHz. Surface current distribution is thoroughly analyzed at both frequencies, showing proper rotation and confirming the antenna's ability to generate strong circular polarization. The antenna also exhibits high radiation efficiency (~87% at 28 GHz and ~82% at 38 GHz) and peak realized gains of 7.5 dBi and 5.5 dBi, respectively. Measured results demonstrate excellent impedance matching, stable radiation patterns, and strong agreement with simulations. The combination of compact size, robust CP performance, and efficient radiation makes the proposed antenna a promising candidate for circularly polarized millimeter-wave systems, including 5G base stations, user equipment, and future high-frequency wireless platforms.

Lien vers l'article

Compact and low mutual coupling 4 × 4 wideband MIMO antenna design for 5G millimeter-wave applications.

Edries M, Mohamed HA, Elsheakh DN, Hekal S. *Sci Rep*. 2026 Mar 25;16(1).

This paper presents a wideband 4 × 4 Multiple-Input-Multiple-Output (MIMO) antenna system operating within the 5G millimeter-wave (mmWave) Frequency Range 2 (FR2). The design targets enhanced mobile broadband (eMBB) applications and features four orthogonally arranged Greek cross-shaped slot antenna (GCSA) elements fed by microstrip lines to effectively reduce mutual coupling and ensure high isolation. Circular edges on the radiating elements are introduced to enhance the impedance bandwidth, while a strategically placed quadrilateral slot in the ground plane optimizes the radiation characteristics. The antenna is fabricated on a Rogers RT/Duroid 4003C substrate (ε(r) = 3.55, thickness = 0.8 mm), resulting in a compact 40 × 40 × 0.8 mm(3) structure. The proposed MIMO system achieves a measured impedance bandwidth of approximately 8 GHz, spanning 24 to 32 GHz at |S(11)|≤ - 10 dB, with a peak gain of 6 dBi at 27.5 GHz. The antenna exhibits directional

radiation patterns perpendicular to the MIMO plane, yielding mutual coupling levels of - 25 dB and - 20 dB at 25 GHz and 29 GHz, respectively. Additionally, the design demonstrates excellent MIMO performance with an Envelope Correlation Coefficient (ECC) < 0.001 and Diversity Gain (DG) ~ 10 dB across the 23.93-31.18 GHz operational band. A comprehensive evaluation of scattering parameters, surface currents, radiation patterns, specific absorption rate (SAR), and diversity metrics confirms the robustness of the proposed design. Prototype measurements closely match the simulated results, validating the antenna's suitability for 5G millimeter-wave communication systems.

Lien vers l'article

Frequency-reconfigurable aperture-coupled magneto-electric dipole antenna for multi-band sub-6 GHz 5G NR systems.

Dastranj A, Shirzad H. *Sci Rep*. 2026 Apr 27.

This paper presents a compact, wideband, and frequency-reconfigurable Magneto-Electric Dipole (MED) antenna designed for sub-6 GHz 5G New Radio (NR) and Industrial, Scientific, and Medical (ISM)/ Wireless Local Area Network (WLAN) applications. The proposed antenna utilizes an aperture-coupled excitation mechanism integrated within a multilayer FR4 structure, featuring complementary electric and magnetic dipole elements that are optimized through a four-step evolutionary design process. The final configuration achieves a simulated broad Impedance Bandwidth (IBW) of 2.24-4.55 GHz in the all-diodes-off state, while maintaining stable broadside radiation, a peak gain of over 7.7 dBi, and a radiation efficiency of up to 94.2%. Frequency reconfigurability is achieved through the use of six strategically placed PIN diodes, which selectively modify the current distribution on the microstrip feed line by coupling six rectangular stubs. Multiple diode-controlled switching states enable wide tunability from 1.79 GHz to 4.41 GHz, providing support for more than twelve major 5G NR bands, including n7, n30, n34, n38, n40, n41, n48, n53, n65, n77, n78, n90, n95, and n97, as well as ISM/WLAN services. Simulated and measured results exhibit strong agreement across all states, with peak gains ranging from 7.06 to 7.82 dBi and radiation efficiencies between 65.6% and 96.1% (see Table 3), confirming the robustness of the aperture-coupled and diode-integrated MED architecture. Compared to recent state-of-the-art MED and reconfigurable MED antennas, the proposed design demonstrates a wider tuning range, competitive gain, and reduced structural complexity while maintaining a compact volume of $0.48\lambda_o \times 0.48\lambda_o \times 0.11\lambda_o$ at 3.5 GHz. These characteristics highlight its suitability for compact 5G terminals, small-cell base stations, reconfigurable wireless systems, and multi-standard communication platforms.

Lien vers l'article

Design and development of a graphene-based MIMO antenna for smart multi-band sub-6 GHz 5G wearable communication applications.

Al-Gburi AJA, Mohammed NJ, Saeidi T, Nurhayati N, Ismail MM. *Sci Rep*. 2026 Apr 4;16(1).

Traditional copper-based planar antennas have traditional disadvantages for wearable applications because of poor flexibility, deteriorated signal under deformation, expensive and environmental problems. To solve these issues, graphene has been proposed as a radiating material with high electrical conductivity, great flexibility, and the possibility of being printed on low-cost textile/paper substrates. In this study, graphene was used as a conductive material in an a two-port MIMO antenna for wearable smart communication. The graphene MIMO wearable antenna is printed on Jeans with a dielectric constant of 1.67, and an overall dimension of 35×55 mm³. The antenna operates in a

multiband mode within the 5G sub-6 GHz spectrum, covering two distinct frequency ranges of 3.1–4.3 GHz and 4.9–6.0 GHz. This makes it a strong candidate for wearable 5G sub-6 GHz terminals, body-centric wireless communication systems, and short-range WLAN/ISM-based smart wearable devices. In addition, higher-order resonant bands at 8.25–9.4 GHz and 10.82–14.4 GHz are observed, indicating that the proposed design inherently exhibits wideband characteristics in the X-band region. The graphene is highly electrically conductive being 4.02 × 10(5) S/m. The SAR analysis was carried out for the entire bandwidth, and it can be seen that energy absorption tends to be more restricted by increasing the skin depth (SC and OC) with higher frequency because of the dependence of dielectric properties on frequency. The maximum measured SARs are quite low below the ICNIRP safety limits 0.84 W/kg averaged over 10 g of tissue at an input power of 0.5 W, and hence it indicates that the proposed graphene-based MIMO configuration is a suitable solution for long-term wearable applications as it does not impose any health threats to the user. SUPPLEMENTARY INFORMATION: The online version contains supplementary material available at 10.1038/s41598-026-42793-5.

Lien vers l'article

Amplitude only nulling of linear antenna arrays for 5G/6G wireless communication by using honey formation optimization.

Akdagli A, Yildiz A, Karaomerlioglu F, Yüksek G, Ekinci S, Izci D, et al. *Sci Rep*. 2026 Apr 10.

This paper presents a new pattern nulling method for linear antenna arrays using the honey formation optimization with a single component (HFOSC) algorithm. HFOSC was validated through extensive tests on 60 benchmark functions, demonstrating superior accuracy and convergence compared to particle swarm optimization (PSO), differential search (DS), moth-flame optimization (MFO), whale optimization algorithm (WOA), and improved grey wolf optimizer (IGWO). The proposed method enables accurate null steering by adjusting only the amplitudes of the array's individual elements while keeping uniform phase and position distributions for a fixed array geometry. A compound cost function including sidelobe levels, null depths, and dynamic range ratios is defined with customized weighting coefficients for the optimization. The HFOSC algorithm performance and feasibility are demonstrated elaborately through illustrative and total numerical simulations based on a 25-element linear array spaced by half-wavelength operating at 28 GHz. The array is synthesized with a 25-dB Chebyshev pattern under single, multiple, and wide null constraints. The simulation results always demonstrate that the proposed optimizer is capable of generating solutions satisfying such contradictory pattern requirements as well as stringent interference suppression constraints to ensure Quality of Service (QoS) and enhance user satisfaction. Thus, this technique is very promising for applications in evolving 5G/6G communication systems.

Lien vers l'article

Architecture réseau

Enhancing 5G uplink communications through efficient PCC-OFDM with neural network-based channel estimation.

J MJ, S S. *Sci Rep*. 2026 Apr 2.

The demand for higher data rates and increased reliability in 5G uplink communications has prompted the exploration of innovative technologies. This paper introduces a novel approach that combines Polynomial-Cancellation-Coded-Orthogonal Frequency Division Multiplexing (PCC-OFDM) and integrates the power of Neural Network based channel estimation. The proposed system aims to optimize spectral efficiency and mitigates the challenges associated with channel estimation in dynamic wireless environments. The proposed system achieves superior error correction capabilities, ensuring robust communication links. The integration of OFDM provides efficient spectrum utilization and enables seamless communication in the presence of fading channels. Furthermore, an Artificial Neural Network- Multilayer Perceptron (ANN-MLP) based channel estimation mechanism is introduced to adaptively learn and predict channel conditions, enhancing the accuracy of estimated channel parameters. The biases and weights of the neural network are optimized by stochastic gradient descent (SGD) approach which in turn minimizes the loss function. Simulation outcomes prove the superior performance of the developed approach, showcasing its potential to revolutionize 5G uplink communications by achieving higher data rates, improved reliability and adaptability to varying channel conditions.

Lien vers l'article

Efficacité énergétique

Reinforcement learning based resource allocation scheme for vehicular communication in 5G networks for smart cities.

Brindha S, Nasreen PPS, Sagar P, Sarma SS. *Sci Rep*. 2026 Apr 2.

With an emphasis on improving energy efficiency (EE) and lowering power consumption of rapidly growing connected vehicles and infrastructures, Vehicle-to-Everything (V2X) communication is emerging as a fundamental element in the development of smart cities. This paper introduces an innovative reinforcement learning (RL)-based method for dynamic resource allocation within 5G-enabled V2X networks, focusing on EE and minimizing power consumption. The suggested framework adeptly modifies transmission power, and spectrum allocation in real-time, responding to fluctuating traffic patterns and network demands. By facilitating ongoing learning and decision-making, the RL system guarantees optimal resource utilization while preserving high-quality service and low-latency communication. Q-learning is employed to dynamically regulate power levels in urban vehicular scenarios, taking Doppler shift, user mobility, and changing traffic conditions into account. Experimental evaluations demonstrate a substantial decrease in power consumption and an improvement in network efficiency providing a sustainable solution for smart mobility initiatives, promoting the advancement of greener, more reliable, and energy-efficient urban transportation systems.

Lien vers l'article

Autres équipements

Smart transparent surfaces for energy-efficient buildings: enabling 5G mmWave connectivity with multispectral compatibility.

Nguyen DT, Shin JH, Kim HJ, Jung CW. *Sci Rep*. 2026 Apr 22.

This paper presents a glass-penetrating transparent surface (GPTS) that provides multispectral compatibility across visible light (VIS), infrared (IR), and ultraviolet (UV) bands, while improving transmission in the 5G millimeter-wave (mmWave) band. For building applications, these techniques are critical to efficiently deploy on-premises mmWave fixed wireless access (FWA) as well as wireless communications with outdoor-to-indoor and indoor-to-outdoor connectivity. To optimize transmission and angular stability, various frequency-selective surface (FSS) designs based on a metallic layer (ML) on glass (GPTS-ML) are first investigated. The ML was then replaced with two types of advanced transparent coatings PEI/Ag/PEDOT:PSS: a transparent electrode (TE) and a low-E (LE) coating with sheet resistances of 9.2 Ω/sq and 5 Ω/sq, respectively. Both structures achieve a transmission loss below 4.7 dB at 28 GHz, while maintaining high VIS transmittance (Tvis) and simultaneously reducing IR transmittance (TIR) and UV transmittance (TUV). GPTS-TE provides Tvis of approximately 66% with balanced TUV of 40% and TIR of 44%, whereas GPTS-LE exhibits stronger IR/UV blocking, with TIR of 19% and TUV of 29.5%, while sustaining low-loss mm-wave transmission. These results illustrate a path towards multi-spectral surface applications that simultaneously support energy efficiency, user comfort, and next generation 5G mmWave FWA services. Our work highlights the potential of transparent metasurfaces as a foundational element in smart buildings and urban communications infrastructure, thereby enabling sustainable and connected living environments.

Lien vers l'article

Applications industrielles

5G communication delay dataset for cloud-based vehicle planning and control.

Zhang X, Xiong L, Zhang P, Feng H, Huang J, Wang X, et al. *Sci Data*. 2026 Apr 15.

Cloud-based intelligent connected vehicles (CICVs) rely on vehicle-to-network-to-vehicle (V2N2V) communication for cooperative planning and control (PnC), where communication delay directly influences control performance and safety. To support research on delay modeling and delay-aware control, we present CICV5G, a publicly available dataset of 5G communication delay for cloud-based CICV applications. The dataset comprises more than 150,000 synchronized records collected from field experiments at the Tongji Intelligent Vehicle Evaluation Base, covering diverse driving environments, network modes, and vehicle velocities. Each record includes network indicators (RSRP, SINR, Cell ID) and vehicle motion data (position, heading, velocity) with millisecond-level timestamps. All measurements were obtained through a real V2N2V loop using a 5G V2N2V testbed with both public and private networks. The dataset has been validated through statistical analysis of delay distributions and network consistency. CICV5G provides a reproducible foundation for developing communication delay models, delay prediction methods, and cloud-based planning and control strategies for CICVs.

Lien vers l'article

Cell Complexity Impact on Railway 5G Performance: Measurements Along Tallinn-Tartu Corridor.

Pilvik R, Jairus T, Sadam A, Kõrbe Kaare K. *Sensors (Basel)*. 2026 Mar 21;26(6).

Fifth-generation (5G) networks enable railway digitalization but face signal degradation challenges in high-mobility environments. While the existing literature attributes degradation primarily to Doppler frequency shifts, this study presents empirical evidence challenging this paradigm. Analysis of 13.7 million 5G New Radio measurements across 370 km of Estonian railway reveals that visible cell density, not velocity, dominates signal quality degradation. Nine geographic hotspots exhibit 5.4-18.0 dB degradation at moderate velocities (54-66 km/h, mean 60.2 km/h) with zero high-speed measurements, excluding the Doppler effect as the reason behind service quality degradation. Cell complexity demonstrates a 3.25× stronger correlation with degradation (r = -0.390) than velocity (r = -0.120), consistent with automatic frequency control tracking instability under high cell ID churn rates (40-115 visible cells per location), though direct confirmation of this mechanism requires access to internal modem frequency-lock state data. Frequency band analysis shows that 700 MHz is optimal at 98.1% of locations, with a 19 dB advantage over 3.5 GHz. Degradation mechanism decomposition reveals within-cell effects (60%, 7.85 dB) and handover boundary effects (40%, 2-6 dB). The findings challenge velocity-centric optimization paradigms and recommend network planning focused on cell overlap reduction rather than Doppler compensation enhancement. Practical recommendations include 700 MHz prioritization, handover parameter optimization, and geographic targeting of identified hotspots for European railway 5G deployment.

Lien vers l'article

Safe and usable ensemble formation for networked medical devices: a comparative study of 5G, NFC and pop-up pairing.

Yilmaz O, Kißmann S, Goschkowski M, Schollmaier P, Beger F, Wieschebrock D, et al. *Int J Comput Assist Radiol Surg*. 2026 Apr 13.

PURPOSE: Incorrectly formed medical device ensembles can cause therapy to be performed at the wrong site or display safety-critical data from the wrong patient. This early, exploratory study investigates which wireless ensemble-creation techniques minimize risk while remaining safe and usable in intraoperative workflows. The goal is to identify the most promising methods among 5G, NFC, and pop-up pairing. METHODS: Eight techniques (5G proximity/location, pop-up pairing, QR Code, Near-Field Communication (NFC) Tag and Reader, device-ID copying, manual selection, device interaction, and SDC context lookup) and five clinical situations (patient bedside, transport, prep room, operating room (OR), post OR) were examined. Five interoperability and clinical experts rated the importance of risk- and usability-related criteria for each situation, as well as how well the criteria are being fulfilled by the different methods. The criteria weights and the method-specific ratings were combined in a quantitative decision matrix to identify the three most promising approaches, which were implemented in a click-dummy prototype and evaluated through formative testing with two clinicians. RESULTS: The analysis rated 5G, NFC, and pop-up pairing the highest when combining all categories. Subsequent formative tests with clinicians from the University Hospital Bonn support technical feasibility and highlight clear trade-offs. In this small sample (n = 2), NFC was perceived as the safest and most preferred technique. 5G offered speed and automation potential, but raised critical concerns regarding accuracy. Pop-up pairing was considered flexible yet error-prone when multiple devices entered pairing mode simultaneously. CONCLUSION: This is a systematic comparison of wireless SDC-ensemble techniques. Early clinical feedback favors NFC for its perceived safety, while 5G and pop-up pairing approaches require additional refinements to mitigate residual risks. As one participant pointed out: "I prefer a reliable and slower over an automated but error-prone method".

Lien vers l'article

Feasibility of robotic telesurgery over wired and private 5 G networks within Brazil's public health system (SUS): a pilot study.

Artifon ELA, Kfouri F, Otoch JP, Kowalski LP, Nahas W, Ebaid G, et al. *Clinics (Sao Paulo)*. 2026 Apr 2;81:100926.

OBJECTIVE: To assess the feasibility and performance of a robotic telesurgery platform operating within the Brazilian Unified Health System (SUS) infrastructure in a dry lab environment under wired and private 5 G network conditions. METHODS: Over three consecutive days, robotic surgeons performed three standardized dry lab tasks from a remote console at PROMIN–FMUSP, with the robotic unit at HU-USP. Sessions were conducted using either a wired or a private 5 G network. Performance outcomes included task success and completion time. Connectivity metrics – latency, jitter and packet loss – were recorded; and per-participant mean values were used in descriptive analyses. Surgeons completed post-session assessments of perceived safety, usability, and mental workload. RESULTS: Twenty-eight robotic surgeons completed dry lab sessions (23 wired, 5 private 5 G). Task success was 100% for Task 1, 82.1% for Task 2, and 89.3% for Task 3; all failures occurred in wired sessions. Median completion times were 26 s (Task 1), 4.5 min (Task 2), and 8.5 min (Task 3). Median latency and jitter were significantly higher in 5 G than in wired sessions (latency: 32.4 vs. 12.0

ms; jitter: 30.8 vs. 6.8 ms). Median packet loss was low under both conditions (0.0% in 5 G; 0.09% in wired). Most surgeons rated the system as safe (78.6% assigned the maximum safety score) and considered it suitable for high-complexity procedures (67.9%). CONCLUSION: Robotic telesurgery within SUS infrastructure was feasible in a simulated environment. Although the private 5 G network exhibited higher latency and jitter than the wired connection, the task completion and usability were preserved, supporting further evaluation in controlled clinical settings.

Lien vers l'article

Evaluation (Mesure des niveaux d'exposition)

Méthodes d'évaluation

Aucun article dans ce bulletin.

Evaluation population générale

Path Loss Dataset from Field Measurements at 3.5 GHz for the Fifth Generation of Wireless Communications in Indoor Environments.

Perdomo-Reyes P, Galvan-Tejada GM, Meneses-Viveros A. *Sci Data*. 2026 Apr 2;13(1).

Wireless communications are today an important mechanism to connect people, machines and things. There are different uses of this technology like security, business, health, education, entertainment, agriculture among many others. In any case, the operational frequency and the scenario where wireless systems are deployed dictate the radio wave propagation conditions and therefore the quality of the communication signals. The path loss refers to the attenuation that wireless signals experiment between pairs of transmitter-receiver and is the basic parameter of performance of wireless communications. In this study, we reported and share different datasets of path loss derived from a campaign of field measurements conducted in three indoor environments. The operational frequency used in this campaign was 3.5 GHz, which is one of the frequency bands of interest for the fifth generation of wireless communications and beyond. The followed strategy to gather data is described in detail, including measurements parameters like equipment, antennas, dimensions and materials of each scenario and the grids used to locate the reception points.

Lien vers l'article

Risques professionnels

Aucun article dans ce bulletin.

Effets biologiques et sur la santé

In silico

Aucun article dans ce bulletin.

In vitro

Biological effects of 5G-modulated 700 MHz RF-EMF exposure on neuronal and glial cell models under isothermal conditions.

Puginier E, Leclercq L, Poulletier de Gannes F, Hurtier A, Orlacchio R, Nabos P, et al. *Sci Rep*. 2026 Mar 28;16(1).

Whether radiofrequency electromagnetic fields (RF-EMF) at wireless telecommunication frequencies can alter brain physiology remains a matter of debate. The 700 MHz band, recently allocated for 4G and early 5G deployment, is increasingly prevalent in the environment, yet its biological effects are poorly documented. Here, we investigated the impact of 700 MHz 5G-modulated RF-EMF exposure on two complementary central nervous system cell models: primary rat cortical astrocytes and human SH-SY5Y neuroblastoma cells. Cells were exposed in transverse electromagnetic (TEM) cells at specific absorption rates (SAR) of 0.08 W/kg and 4 W/kg, for 1 h or 24 h, and analyzed immediately or after a 24 h recovery period. Multiparametric flow cytometry quantified mitochondrial reactive oxygen species (ROS), cell viability, and apoptosis stratified as early and late, together with astrocytes' proliferation. Across all exposure conditions, no statistically significant differences were detected compared to sham controls, while positive controls with hydrogen peroxide elicited significant increases in ROS and apoptosis, validating assay sensitivity. These results demonstrate that, under strictly controlled iso-thermal conditions, 5G-modulated 700 MHz RF-EMF exposure does not induce measurable oxidative stress, apoptosis, or proliferative alterations in astrocytic and neuronal models. Our findings provide evidence supporting the absence of acute or subacute biological effects in vitro at isothermal exposure levels up to 4 W/kg, thereby reinforcing the scientific basis for current exposure guidelines.

Lien vers l'article

Sur l'animal

Effect of high-frequency radiofrequency (6 GHz) electromagnetic radiation on oxidative stress and kidney morphology.

Emre M, Karamazi Y, Emre T, Varan NE, Toyran T, Yücebilgiç G. *Toxicol Ind Health*. 2026 Apr;42(4):124-36.

This study aimed to investigate the effects of high-frequency (6 GHz) radiofrequency electromagnetic radiation (RF-EMR) exposure on oxidative stress markers and kidney morphology. Our study was designed with 3 groups, each containing 10 animals. These groups were: control, sham, and RF-EMR

exposed group. No treatment was applied to the control group; the sham group was housed in the same room under the same conditions and for equal periods of time, except that the generator was turned off. The RF-EMR exposed group was exposed to 6 GHz RF-EMR emitted from the signal generator for 4 hours per day for 6 weeks. At the end of the experimental period, intracardiac blood was collected from animals and plasma oxidant (MDA), antioxidant (SOD, CAT and GSH) and cortisol markers were analyzed. After, the rats in all groups were sacrificed and kidney tissues were removed. Hematoxylin and eosin staining methods were applied histopathologically. Blood-plasma GSH, CAT, SOD and MDA levels (excluding cortisol) were lower in the RF-EMR exposed group compared to the control and sham groups ($p < .001$). No significant difference was observed in plasma levels GSH, CAT, SOD, MDA and cortisol activities between control and sham groups. In addition, we reported that the histological characteristics of kidney tissue were affected by RF-EMR. The results of our study indicated that 6 GHz RF-EMR can function as an environmental stress factor and can modulate oxidative stress in blood plasma and cause morphological changes in kidney tissue.

Lien vers l'article

Sur l'homme

Near-field and far-field exposures to radiofrequency electromagnetic fields and cancer risks in humans: a protocol for an umbrella review of epidemiological studies.

Ziegler JL, Lagorio S, Mattsson MO, Zeni O, Bolte J, Ledent M, et al. *Syst Rev*. 2026 Mar 12;15(1).

BACKGROUND: Exposure to radiofrequency electromagnetic fields (RF-EMF; frequencies 100 kHz to 300 GHz) is ubiquitous. As the use of RF-EMF has grown steadily since the 1950s due to advances in telecommunications and other technologies, concerns about potential health effects have persisted. The World Health Organization (WHO) identified key areas of concern, with cancer being most frequently rated as critical. To synthesize evidence on the association between RF-EMF exposure and neoplastic diseases, we will carry out two separate umbrella reviews to account for different RF-EMF exposure conditions: one will focus on near-field exposure and the other on far-field exposure. Both umbrella reviews will include RF-EMF exposure in living and occupational settings. METHODS: Systematic reviews and meta-analyses of human observational studies on RF-EMF and cancer were searched in MEDLINE, Web of Science Core Collection, EMF-Portal, and Epistemonikos databases. Eligibility criteria will follow the PECOS (Population, Exposure, Comparator, Outcome, Study type) scheme. Eligibility and quality of the identified articles will be evaluated by two reviewers independently. The tools AMSTAR 2 (A MeaSurement Tool to Assess systematic Reviews) and ROBIS (Risk of Bias in Systematic Reviews) will be used to systematically assess methodological quality and risk of bias. Data will be extracted and summarized in a qualitative synthesis using standardized forms and presented in text and tables. DISCUSSION: These umbrella reviews aim to offer a comprehensive overview of the topic by including systematic reviews and meta-analyses that studied cancer-related health effects of near-field and far-field RF-EMF exposure. In addition, a risk of bias rating will be performed to assess the quality of existing systematic reviews and meta-analyses in the field. SYSTEMATIC REVIEW REGISTRATION: PROSPERO CRD42024529007.

Lien vers l'article

Cancer incidence in telecommunication and broadcasting workers in the United Kingdom: Preliminary analysis of the National Register of RF Workers.

Litchfield I. *Int J Hyg Environ Health*. 2026 May;274:114785.

OBJECTIVES: There is a broadly acknowledged need for more robust research exploring the potential health effects of occupational radiofrequency radiation (RF) exposure. The National Register of RF Workers is a long-standing database consisting of workers that typically work outside and are occupationally exposed to RF in the telecommunication and broadcast industries in the United Kingdom. This work describes the initial preliminary analysis of the cohort comparing cancer incidence at multiple sites with that observed in the general population. METHODS: Cancer registration (incidence) details from NHS Digital were used and standardised registration rates (SRR) calculated as the ratio of observed to expected numbers of registrations expressed as a percentage. In calculating P-values and confidence intervals, it was assumed that registrations occurred following a Poisson distribution. All significance tests were two-tailed. RESULTS: The cohort comprised 1777 employees (1744 males and 33 females) Compared with national rates, all cancers combined are slightly below expectation (Observed 39, SRR 93). The only statistically significant finding is for an excess of skin cancer (excluding melanoma) (Observed 25, SRR 177, 95% CI 117 to 258, $P < 0.01$). CONCLUSIONS: Amongst legitimate concerns over the health effects of long-term occupational exposure to RF in the telecommunication and broadcast sector it is important not to overlook the significant hazard of exposure to ultraviolet radiation in a workforce that predominantly works outside. There are several ways organisations might mitigate this impact including amending working hours during the summer months and culturally tailored education on the importance of individual preventative measures.

Lien vers l'article

No thermal skin effects at environmental 26 GHz field strengths relevant to 5G deployment.

Michelant L, Delanaud S, Hugueville L, Leveque P, Bach V, Tourneux P, et al. *Sci Rep*. 2026 Apr 27.

The deployment of 5G millimeter wave technology at 26 GHz raises questions about potential thermal effects on human tissues. Controlled human studies examining millimeter wave thermal responses remain limited. We investigated the effects of acute 26 GHz exposure on skin temperature in healthy volunteers under controlled laboratory conditions. Thirty-one healthy young adults participated in a triple-blind, randomized, crossover study. Participants underwent genuine 26 GHz exposure (2 V/m at head level, 1 V/m at torso level) and sham exposure, each lasting 26 minutes 30 seconds. Skin temperature was continuously monitored using infrared thermography at five anatomical regions (face, bilateral hand dorsum, bilateral infraclavicular areas) across three experimental phases. No statistically significant thermal effects were detected, with no main effect of exposure condition for any skin region (all $p > 0.34$). No significant exposure-phase interactions were detected for any measurement (all $p > 0.09$). Progressive decreases in distal skin temperatures (exceeding 1.5°C, $p < 0.0001$) occurred independently of exposure condition, reflecting normal thermoregulatory adaptation to seated immobility. Distal-proximal gradient analysis showed no significant difference between conditions (right: $p = 0.332$; left: $p = 0.319$), and bilateral comparisons revealed no thermal asymmetry ($p = 0.269$). These findings provide reassuring evidence that acute 26 GHz exposure at environmental field strengths produces no detectable thermal effects in healthy young adults, at levels substantially below ICNIRP reference limits. However, these results should not be interpreted as a direct validation of those guideline threshold values.

Lien vers l'article

Recording the extremely low frequency pulsations of wireless communication electromagnetic fields.

Panagopoulos DJ, Litovsky R, Chamberlin K. *Electromagn Biol Med*. 2026 Apr 19:1-10.

All digital Wireless Communication (WC) electromagnetic field (EMF)/radiation (EMR) signals (from mobile/"smart" phones and corresponding base antennas, cordless domestic phones, Wireless Fidelity (Wi-Fi) routers, "Bluetooth" wireless connection among electronic devices, etc.) are emitted discontinuously, in the form of on/off pulses repeated at various Extremely Low Frequency (ELF) rates. Yet, many scientists ignore/underestimate these ELF pulsations, and characterize all WC emissions simply as Radio Frequency (RF)/Microwave (MW) signals. Here, we provide recordings of ELF pulsations with respect to time, emitted by the most common WC devices, specifically Wi-Fi router, 4(th) and 5(th) Generation (4G, 5G) mobile phones. We used a broadband antenna, connected to an RF spectrum analyzer (SA), calibrated the SA at the signal's carrier MW frequency and recorded the power of the final emitted RF/MW signal with respect to time. We recorded emissions at 10 ms, 100 ms, 1 s, and 2 s sweep times, capturing the pulses repeated at various ELF rates, clearly showing the ELF pulsing emissions from the WC devices. As in all real WC EMF signals emitted by commercially available devices and corresponding antennas, there is intense variability in the amplitude, shape, duration, and repetition frequency of the pulses. The present study, in combination with the Ion Forced Oscillation and Voltage-Gated Ion Channel (IFO-VGIC) mechanism of non-thermal EMF-bioeffects, imply that the non-thermal biological and health effects of WC EMFs are induced by the ELF pulsation, modulation and variability, and not by the standalone (non-modulated) RF carrier wave EMFs which can produce only heating.

Lien vers l'article

Reproduction

Aucun article dans ce bulletin.

Dispositifs médicaux implantables

Aucun article dans ce bulletin.